

Asymptotic System Performance over Generalized Fading Channels with Application to Maximal-Ratio Combining

Francisco Raimundo Albuquerque Parente¹, *Student Member, IEEE*, Flavio du Pin Calmon², *Member, IEEE*,
and José Cândido Silveira Santos Filho³, *Member, IEEE*

Abstract—The performance of wireless communications systems is affected by many aspects of the fading phenomenon, such as clustering, nonlinearity, scattered waves, and line of sight. Even though several fading models exist which address a multitude of propagation conditions, in many cases the fading statistics or the associated system performance cannot be obtained in a closed form. In such cases, it is difficult to decipher how each physical aspect of fading impacts the system performance. In this work, we propose a unified asymptotic characterization at high signal-to-noise ratio to obtain simple, general closed-form expressions for the diversity and coding gains of essential performance metrics, namely, symbol error rate and outage probability. We cover generalized propagation conditions and all the referred fading aspects. The analysis is further extended to investigate the performance of multibranch maximal-ratio combining. Capitalizing on the fact that the asymptotic channel distribution around the origin fully determines the diversity and coding gains, our results provide new insights into how each physical aspect of fading ultimately affects the wireless system performance.

Index Terms—Asymptotic performance, error rate, fading channels, maximal-ratio combining, outage probability.

I. INTRODUCTION

Wireless communications are entering into a new era. The emerging fifth generation (5G) of mobile networks promises ubiquitous high-rate, low-latency, and ultra-reliable communications [2]–[4]. In order to meet such unprecedented system requirements, 5G and its key technologies can benefit from a proper modeling of the radio channel that enables an accurate description of the multipath fading phenomena [5]–[8]. The wireless system performance is impacted by several elements of fading, including clustering, nonlinearity, scattered waves, and line of sight. Different combinations of these elements have been incorporated into various probabilistic fading models, ranging from the simple one-parameter

Rayleigh distribution to the ultrageneralized seven-parameter α - η - κ - μ distribution [7]. With these models, one can assess the performance of communications systems in terms of metrics such as symbol error probability (SEP) and outage probability (OP), ultimately helping optimize the design of emerging 5G wireless networks.

For many fading scenarios, an exact performance analysis is intricate, and it usually does not offer tractable closed-form solutions [9]–[11]. The analysis becomes even more complicated when there are multiple links connecting source to destination, such as in diversity-combining schemes. For example, selection combining (SC), equal-gain combining (EGC), and maximal-ratio combining (MRC) are popular diversity techniques whose analysis in terms of SEP and OP is cumbersome for generalized fading conditions [10], [12]. Because of that, it is difficult to obtain insights on how each fading aspect impacts the system performance. This problem can be overcome via an asymptotic performance analysis at high signal-to-noise ratio (SNR), a condition required in practice for many wireless applications. Song et al. [13] derived asymptotic closed-form expressions for the SEP and OP of multibranch diversity schemes, namely, SC, EGC, MRC, and hybrid techniques, all of them operating over Rician channels. Considering a more general fading scenario, Zhu et al. [10] derived asymptotic upper and lower bounds for SEP and OP of diversity receivers operating over the α - μ fading model. More recently, based on the extreme-value theory, Al-Badarneh et al. [12] obtained the asymptotic performance characterization for the k th best link selection over some fading channels, namely, Weibull, gamma, α - μ , and gamma-gamma. Although covering different propagation conditions, these works exploited the asymptotic approach on a case-by-case basis, constrained to certain fading scenarios. To our best knowledge, no published work provides comprehensive insights on how each physical aspect of fading impacts intricate 5G-like channels.

In this work we aim to shed light on how each physical aspect of multipath fading impacts the wireless system performance. To this end, we provide simple, general, and unified closed-form expressions for the high-SNR SEP and OP of communications systems operating in a broad family of Gaussian-class fading scenarios. Following standard practice, we describe our expressions in terms of two key asymptotic parameters: the diversity and coding gains. The

F. R. A. Parente and J. C. S. Santos Filho are with the Department of Communications, School of Electrical and Computer Engineering, University of Campinas (UNICAMP), Campinas, SP 13083-852, Brazil (e-mails: parente@decom.fee.unicamp.br, candido@decom.fee.unicamp.br).

Flavio du Pin Calmon is with the School of Engineering and Applied Sciences, Harvard University, Cambridge, MA 02138, United States (e-mail: fcalmon@g.harvard.edu).

This work was supported by the São Paulo Research Foundation (FAPESP) under Grant 2018/25009-4.

This article is an extended *invited paper* of a preliminary work presented in XXXVII Brazilian Symposium on Telecommunications and Signal Processing (SBRT'19), Petrópolis, RJ, Brazil, Sep./Oct., 2019 [1].

Digital Object Identifier: 10.14209/jcis.2020.18

covered scenarios include as special cases a large number of fading models, ranging from the Rayleigh distribution to the α - η - κ - μ distribution, and embracing all the referred fading aspects, namely, clustering, nonlinearity, scattered waves, and line of sight. Our approach capitalizes on an important finding in [11]: the high-SNR SEP and OP depend exclusively on the asymptotic channel distribution around the origin. Therefore, our main challenge here is to find a comprehensive asymptotic channel distribution that encompasses the broad class of fading scenarios under investigation. After obtaining such characterization, we extend the analysis to investigate the asymptotic performance of multibranch diversity receivers operating over generalized fading channels. In particular, we apply the analysis to the MRC scheme, which is the optimal linear diversity-combining technique [14]. We demonstrate that all the aforementioned fading aspects impact the coding gain, whereas only clustering and nonlinearity impact the diversity gain.

The remainder of this paper is organized as follows. Section II revisits key results from the literature to provide some preliminaries for our work. In Section III we develop an asymptotic analysis to obtain a comprehensive characterization of the system performance at high SNR. Section IV reduces the proposed general model to many particular cases and provides closed-form expressions for the diversity and coding gains of a variety of fading models. In Section V the proposed asymptotic characterization is further extended to address multibranch MRC receivers. In Section VI we evaluate the diversity and coding gains in terms of the fading parameters for single-branch and multibranch MRC receivers. Finally, Section VII summarizes the main conclusions of this paper.

In what follows, $f_{(\cdot)}(\cdot)$ denotes probability density function (pdf); $\mathbb{E}[\cdot]$, expected value; $\mathbb{V}[\cdot]$, variance; $(\cdot)^T$, transpose; $\log[\cdot]$, the base-10 logarithm; $\Gamma(\cdot)$, the gamma function; $Q(x) \triangleq \int_x^\infty (1/\sqrt{2\pi}) \exp(-t^2/2) dt$, the Q -function; and “ \sim ”, asymptotically equal to around zero, i.e., $f(x) \sim g(x) \iff \lim_{x \rightarrow 0} f(x)/g(x) = 1$.

II. PRELIMINARIES

Two metrics commonly used to assess the wireless system performance are the SEP and OP, whose formulation relies on the probability distribution of the (fading) channel. In [11], Wang and Giannakis demonstrated that at high SNR the SEP and OP can be characterized by diversity and coding gains that depend exclusively on the asymptotic channel power pdf around the origin. We now revisit how this asymptotic pdf fully determines the high-SNR behavior of SEP and OP.

Let $B \geq 0$ represent the channel power coefficient with asymptotic pdf given by

$$f_B(\beta) \sim a_{B,0} \beta^{b_{B,0}}, \quad (1)$$

where $a_{B,0}$ and $b_{B,0}$ are constants obtained from the first term of the Maclaurin series expansion of $f_B(\cdot)$. Considering $\gamma = B\bar{\gamma}$ to be the instantaneous SNR at the receiver, it follows that $\bar{\gamma}$ is the mean SNR when $\mathbb{E}[B] = 1$. We assume additive white Gaussian noise (AWGN) and an instantaneous SEP in

the form of $Q(\sqrt{\nu B\bar{\gamma}})$, where ν is a positive constant that depends on the signaling scheme. Accordingly, the average SEP (P_E) can be expressed at high SNR as [11]

$$P_E \sim (G_c \bar{\gamma})^{-G_d}, \quad (2)$$

where the diversity gain G_d and the coding gain G_c are obtained in terms of $a_{B,0}$ and $b_{B,0}$ as

$$G_d = b_{B,0} + 1 \quad (3a)$$

$$G_c = \nu \left[\frac{2^{b_{B,0}} a_{B,0} \Gamma(b_{B,0} + 3/2)}{\sqrt{\pi} (b_{B,0} + 1)} \right]^{-\frac{1}{b_{B,0} + 1}}. \quad (3b)$$

In a similar manner, the OP (P_{out}) can be expressed at high SNR as [11]

$$P_{\text{out}} \sim (O_c \bar{\gamma})^{-O_d}, \quad (4)$$

where the diversity gain O_d and the coding gain O_c are obtained as

$$O_d = G_d = b_{B,0} + 1 \quad (5a)$$

$$O_c = \frac{1}{\gamma_{\text{th}}} \left(\frac{a_{B,0}}{b_{B,0} + 1} \right)^{-\frac{1}{b_{B,0} + 1}}, \quad (5b)$$

and $\gamma_{\text{th}} > 0$ is a certain outage threshold of SNR.

Besides the system parameters ν and γ_{th} , note that the diversity and coding gains of SEP and OP only depend on the terms $a_{B,0}$ and $b_{B,0}$ of the asymptotic channel power pdf around the origin. If $a_{B,0}$ and $b_{B,0}$ are expressed in terms of the aforementioned fading aspects, we can outline how each fading parameter affects the system performance. To this end, we introduce next a novel asymptotic analysis that leads to $a_{B,0}$ and $b_{B,0}$ in terms of the physical parameters embraced by generalized fading models.

III. ASYMPTOTIC ANALYSIS

In this section, we develop an asymptotic analysis considering a general fading scenario to reveal how physical parameters impact the high-SNR system performance in a broad class of fading conditions.

A. General Fading Model

The signal transmitted over a multipath fading channel reaches the receiver in a large number of scattered, reflected, and diffracted waves, coming from diverse paths and with random amplitudes. In many physical situations, these amplitudes can be assumed statistically independent and with finite variances, such that the conditions of the Central Limit Theorem are satisfied [15], [16]. Accordingly, the sum of these amplitudes at the receiver yields a Gaussian random variable (RV), which has motivated many Gaussian-class fading models (e.g., see [7], [17], [18], and references therein).

Following standard practice [7], we consider a general fading model obtained from a sum of squared independent Gaussian RVs. This way, the channel power B can be written as

$$B^{\frac{\alpha}{2}} = \sum_{i=1}^M X_i^2 \triangleq S, \quad (6)$$

where $\alpha > 0$ is a nonlinearity parameter [7], M is the number of Gaussian components, and each X_i is a Gaussian RV with mean $\mathbb{E}[X_i] = m_i$ and variance $\mathbb{V}[X_i] = \sigma_i^2$. We can arrange the components X_i into the vector form $\mathbf{X} \triangleq [X_1 \ X_2 \ \cdots \ X_M]^T$ so that the multivariate pdf of \mathbf{X} , $f_{\mathbf{X}}(\cdot)$, can be formulated in terms of its mean vector $\mathbf{m} \triangleq \mathbb{E}[\mathbf{X}]$ and covariance matrix $\mathbf{\Sigma} \triangleq \mathbb{E}[(\mathbf{X} - \mathbf{m})(\mathbf{X} - \mathbf{m})^T]$. Specifically, the (positive-definite) covariance matrix $\mathbf{\Sigma}$ can be expressed as

$$\mathbf{\Sigma} = \begin{bmatrix} \sigma_1^2 & 0 & \cdots & 0 \\ 0 & \sigma_2^2 & \cdots & 0 \\ \vdots & \vdots & \ddots & \vdots \\ 0 & 0 & \cdots & \sigma_M^2 \end{bmatrix}, \quad (7)$$

whose inverse is given by

$$\mathbf{\Sigma}^{-1} = \begin{bmatrix} \frac{1}{\sigma_1^2} & 0 & \cdots & 0 \\ 0 & \frac{1}{\sigma_2^2} & \cdots & 0 \\ \vdots & \vdots & \ddots & \vdots \\ 0 & 0 & \cdots & \frac{1}{\sigma_M^2} \end{bmatrix}. \quad (8)$$

Altogether, the multivariate Gaussian pdf of \mathbf{X} can be obtained as

$$f_{\mathbf{X}}(\mathbf{x}) = \frac{\exp\left[-\frac{1}{2}(\mathbf{x} - \mathbf{m})^T \mathbf{\Sigma}^{-1}(\mathbf{x} - \mathbf{m})\right]}{[(2\pi)^M \det(\mathbf{\Sigma})]^{\frac{1}{2}}}. \quad (9)$$

Considering this general fading model, next we determine the asymptotic channel power pdf.

B. Asymptotic Channel Characterization

We now obtain the asymptotic pdf of $B = S^{2/\alpha}$. To this end, we initially derive the asymptotic pdf of \mathbf{X} , of $\mathbf{X}^2 \triangleq [X_1^2 \ X_2^2 \ \cdots \ X_M^2]^T$, and of S .

Using the Maclaurin series expansion of the exponential function in (9) and taking its first term, the asymptotic pdf of \mathbf{X} can be written as

$$f_{\mathbf{X}}(\mathbf{x}) \sim \frac{\exp\left[-\frac{1}{2}\mathbf{m}^T \mathbf{\Sigma}^{-1} \mathbf{m}\right]}{[(2\pi)^M \det(\mathbf{\Sigma})]^{\frac{1}{2}}}. \quad (10)$$

For convenience, we let $k_i \triangleq m_i^2/\sigma_i^2$, $\forall i$, such that (10) reduces to

$$f_{\mathbf{X}}(\mathbf{x}) \sim (2\pi)^{-\frac{M}{2}} \exp\left[-\frac{1}{2}\sum_{i=1}^M k_i\right] \prod_{i=1}^M \frac{1}{\sigma_i}. \quad (11)$$

Furthermore, via a simple transformation of variables, we obtain from (11) the asymptotic pdf of \mathbf{X}^2 :

$$f_{\mathbf{X}^2}(\mathbf{x}^2) \sim (2\pi)^{-\frac{M}{2}} \exp\left[-\frac{1}{2}\sum_{i=1}^M k_i\right] \prod_{i=1}^M \frac{1}{\sigma_i |x_i|}. \quad (12)$$

In order to obtain from (12) the asymptotic pdf of S (defined in (6)), let the Maclaurin series expansion of the pdf of each X_i^2 be given by

$$f_{X_i^2}(x_i^2) = \sum_{n=0}^{\infty} a_{i,n} (x_i^2)^{b_{i,n}} \sim a_{i,0} (x_i^2)^{b_{i,0}}, \quad (13)$$

and the Maclaurin series expansion of the pdf of S be expressed by

$$f_S(s) = \sum_{n=0}^{\infty} a_n s^{b_n} \sim a_0 s^{b_0}, \quad (14)$$

where $a_{i,n}$, a_n , $b_{i,n}$, and b_n are constants, $\forall i, n$. Note that $a_{i,0} (x_i^2)^{b_{i,0}}$ and $a_0 s^{b_0}$ denote the asymptote of $f_{X_i^2}(\cdot)$ and of $f_S(\cdot)$, respectively. Since the asymptotic multivariate pdf of independent RVs is equal to the product of the corresponding asymptotic marginal pdfs [19], we have that

$$f_{\mathbf{X}^2}(\mathbf{x}^2) \sim \prod_{i=1}^M a_{i,0} (x_i^2)^{b_{i,0}}. \quad (15)$$

In this way, comparing (15) with (12), we obtain $a_{i,0}$ and $b_{i,0}$ as

$$a_{i,0} = (2\pi)^{-\frac{1}{2}} \exp\left[-\frac{1}{2M}\sum_{j=1}^M k_j\right] \prod_{j=1}^M \sigma_j^{-\frac{1}{M}} \quad (16a)$$

$$b_{i,0} = -\frac{1}{2}, \quad (16b)$$

and substituting (16) into [19, eq. (23)], we attain

$$a_0 = \frac{\exp\left[-\frac{1}{2}\sum_{i=1}^M k_i\right]}{2^{\frac{M}{2}} \Gamma\left(\frac{M}{2}\right)} \prod_{i=1}^M \frac{1}{\sigma_i} \quad (17a)$$

$$b_0 = \frac{M}{2} - 1. \quad (17b)$$

Finally, we obtain the asymptotic pdf of $B = S^{2/\alpha}$ by performing once again a transformation of variables, which leads to

$$f_B(\beta) \sim a_{B,0} \beta^{b_{B,0}} = \frac{\alpha a_0}{2} \beta^{\frac{\alpha(b_0+1)-2}{2}}. \quad (18)$$

Using (17) and (18), $a_{B,0}$ and $b_{B,0}$ are then expressed as

$$a_{B,0} = \alpha \frac{\exp\left[-\frac{1}{2}\sum_{i=1}^M k_i\right]}{2^{\frac{M+2}{2}} \Gamma\left(\frac{M}{2}\right)} \prod_{i=1}^M \frac{1}{\sigma_i} \quad (19a)$$

$$b_{B,0} = \frac{\alpha M}{4} - 1. \quad (19b)$$

Note that (19) gives the terms $a_{B,0}$ and $b_{B,0}$ as a function of the physical parameters M , α , $\{m_i\}_{i=1}^M$, and $\{\sigma_i^2\}_{i=1}^M$ from the general fading model in (6). We can now obtain a comprehensive characterization of the asymptotic system performance in terms of these fading parameters, as provided next.

C. Diversity and Coding Gains

Based on the above analysis, we can use (19) to obtain the diversity and coding gains for SEP and OP, thereby providing an insightful system performance characterization.

Accordingly, substituting (19) into (3), we obtain the gains for SEP:

$$G_d = \frac{\alpha M}{4} \quad (20a)$$

$$G_c = \nu \left\{ M \pi^{\frac{1}{2}} 2^{\frac{M}{2}(1-\frac{\alpha}{2})} \Gamma\left(\frac{M}{2}\right) \left[\Gamma\left(\frac{\alpha M}{4} + \frac{1}{2}\right) \right]^{-1} \right. \\ \left. \times \exp\left[\frac{1}{2} \sum_{i=1}^M k_i \right] \prod_{i=1}^M \sigma_i \right\}^{\frac{4}{\alpha M}}. \quad (20b)$$

Similarly, substituting (19) into (5), we obtain the gains for OP:

$$O_d = G_d = \frac{\alpha M}{4} \quad (21a)$$

$$O_c = \frac{1}{\gamma_{th}} \left\{ M 2^{\frac{M}{2}-1} \Gamma\left(\frac{M}{2}\right) \exp\left[\frac{1}{2} \sum_{i=1}^M k_i \right] \prod_{i=1}^M \sigma_i \right\}^{\frac{4}{\alpha M}}. \quad (21b)$$

For any values of ν and γ_{th} , note from (20) and (21) that the diversity and coding gains of SEP and OP are given in terms of the various elements of the fading model in (6): the number of multipath clusters (M), the medium nonlinearity (α), the line of sight (m_i), and the mean power of the scattered waves (σ_i^2). Therefore, we have a simple and thorough understanding about how each fading parameter impacts the system performance at high-SNR conditions, a compelling regime to assess and compare communications systems.

IV. PARTICULAR CASES

The general fading model considered in the previous section can be reduced to a variety of existing fading distributions. Before doing so, we address the case where the multipath clusters X_i in (6) are exchangeable RVs [15], which we call commutative scenario.

A. Commutative Scenario

In this scenario, the RVs X_i in (6) are identically distributed. Under such constraint, we can eliminate the indices to let $m_i = m$, $\sigma_i = \sigma$, and $k_i = k$, $\forall i$. Using this into (20) and (21), the diversity and coding gains reduce to

$$G_d = O_d = \frac{\alpha M}{4} \quad (22a)$$

$$G_c = \nu \left\{ \sigma^M M \pi^{\frac{1}{2}} 2^{\frac{M}{2}(1-\frac{\alpha}{2})} \Gamma\left(\frac{M}{2}\right) \left[\Gamma\left(\frac{\alpha M}{4} + \frac{1}{2}\right) \right]^{-1} \right. \\ \left. \times \exp\left[\frac{kM}{2} \right] \right\}^{\frac{4}{\alpha M}} \quad (22b)$$

$$O_c = \frac{1}{\gamma_{th}} \left\{ \sigma^M M 2^{\frac{M}{2}-1} \Gamma\left(\frac{M}{2}\right) \exp\left[\frac{kM}{2} \right] \right\}^{\frac{4}{\alpha M}}. \quad (22c)$$

From these expressions, we provide in Section VI some insights into the system performance in terms of each fading parameter. Previously, we reduce (20) and (21) to many existing fading models, as detailed next.

B. Existing Fading Models

There are many distributions available in the literature that model the fading channel. In order to reduce our analysis to each specific case, we follow a common notation [7] and define some parameters:

- $K > 0$ is the ratio between the total power of the specular components and the total power of the scattered components, i.e.,

$$K \triangleq \frac{\sum_{i=1}^M m_i^2}{\sum_{i=1}^M \sigma_i^2}; \quad (23)$$

- $P > 0$ is the ratio between the number of in-phase components M_x and the number of quadrature components M_y , i.e.,

$$P \triangleq \frac{M_x}{M_y}, \quad (24)$$

where $M = M_x + M_y$;

- $Q > 0$ is the ratio between two other ratios, namely, (i) the total power of the in-phase specular components divided by the total power of the in-phase scattered components ($K_x \triangleq \frac{\sum_{i=1}^{M_x} m_i^2}{\sum_{i=1}^{M_x} \sigma_i^2}$) and (ii) the total power of the quadrature specular components divided by the total power of the quadrature scattered components ($K_y \triangleq \frac{\sum_{i=M_x+1}^{M_x+M_y} m_i^2}{\sum_{i=M_x+1}^{M_x+M_y} \sigma_i^2}$), i.e.,

$$Q \triangleq \frac{K_x}{K_y}. \quad (25)$$

Table I presents the gains for many fading models, from the simple Rayleigh distribution to the highly sophisticated α - η - κ - μ distribution. As a user guide to the reader, we provide a detailed explanation of that table:

- The first column outlines several popular Gaussian-class fading models available in the literature. All these models can be obtained from (6) as particular cases;
- The second column provides the parameters of the corresponding fading model in the first column;
- The third column shows how to set the parameters of the general model in (6) in order to match each existing model. Such correspondence is in terms of the parameters M , K , P , Q , α , and σ , where parameters not shown are either irrelevant for the equivalence (e.g., Q is not a parameter of the Rayleigh distribution) or the same for our general model and its corresponding particular case (e.g., the nonlinearity parameter α is the same for the general fading model and the α - μ fading model). Furthermore, $\{(X_i, m_i, \sigma_i)\}_{i=1}^{M_x}$ denotes the Gaussian clusters and parameters of the in-phase components, whereas $\{(X_i, m_i, \sigma_i)\}_{i=M_x+1}^{M_x+M_y}$ denotes the Gaussian clusters and parameters of the quadrature components.
- The fourth column provides closed-form expressions for the diversity gains of SEP and OP ($G_d = O_d$) in terms of the original parameterization (in the second column);
- The fifth and sixth columns provide, respectively, closed-form expressions for the coding gains of SEP (G_c) and OP (O_c), also in terms of the original parameterization.

TABLE I
DIVERSITY AND CODING GAINS FOR EXISTING FADING MODELS

Fading Model	Original Parameterization ^a	General Model Parameterization	$G_d = O_d$	G_c	O_c
Rayleigh	(Ω)	$M = 2; K = 0; P = 1; \alpha = 2;$ $\sigma_1 = \sigma_2 = \left[\frac{\Omega}{2}\right]^{\frac{1}{2}}.$	1	$2\nu\Omega$	$\frac{\Omega}{\gamma_{th}}$
Hoyt	(b, Ω)	$M = 2; K = 0; P = 1; \alpha = 2;$ $\sigma_1 = \left[\frac{\Omega(1+b)}{2}\right]^{\frac{1}{2}}; \sigma_2 = \left[\frac{\Omega(1-b)}{2}\right]^{\frac{1}{2}}.$	1	$2\nu\Omega [(1+b)(1-b)]^{\frac{1}{2}}$	$\frac{\Omega}{\gamma_{th}} [(1+b)(1-b)]^{\frac{1}{2}}$
Rice	(k_{Rice}, Ω)	$M = 2; K = k_{Rice}; P = 1; \alpha = 2;$ $\sigma_1 = \sigma_2 = \left[\frac{\Omega}{2(k_{Rice} + 1)}\right]^{\frac{1}{2}}.$	1	$2\nu\Omega \frac{\exp[k_{Rice}]}{k_{Rice} + 1}$	$\frac{\Omega}{\gamma_{th}} \frac{\exp[k_{Rice}]}{k_{Rice} + 1}$
Nakagami- m	(m, Ω)	$M = 2m; K = 0; P = 1; \alpha = 2;$ $\sigma_i = \left[\frac{\Omega}{2m}\right]^{\frac{1}{2}}, \forall i \in \{1, \dots, M\}.$	m	$\frac{\nu\Omega}{2} \left[\frac{2\sqrt{\pi}\Gamma(m)}{m^{m-1}\Gamma(m + \frac{1}{2})}\right]^{\frac{1}{m}}$	$\frac{\Omega}{\gamma_{th}} \left[\frac{\Gamma(m)}{m^{m-1}}\right]^{\frac{1}{m}}$
Weibull	(α, Ω)	$M = 2; K = 0; P = 1;$ $\sigma_1 = \sigma_2 = \left[\frac{\Omega}{2}\right]^{\frac{1}{2}}.$	$\frac{\alpha}{2}$	$\frac{\nu}{2} \left[\frac{2\sqrt{\pi}\Omega}{\Gamma(\frac{\alpha}{2} + \frac{1}{2})}\right]^{\frac{2}{\alpha}}$	$\frac{\Omega^{\frac{2}{\alpha}}}{\gamma_{th}}$
α - μ	(α, μ, \hat{r})	$M = 2\mu; K = 0; P = 1;$ $\sigma_i = \left[\frac{\hat{r}^\alpha}{2\mu}\right]^{\frac{1}{2}}, \forall i \in \{1, \dots, M\}.$	$\frac{\alpha\mu}{2}$	$\frac{\nu\hat{r}^2}{2} \left[\frac{2\sqrt{\pi}\Gamma(\mu)}{\mu^{\mu-1}\Gamma(\frac{\alpha\mu}{2} + \frac{1}{2})}\right]^{\frac{2}{\alpha\mu}}$	$\frac{\hat{r}^2}{\gamma_{th}} \left[\frac{\Gamma(\mu)}{\mu^{\mu-1}}\right]^{\frac{2}{\alpha\mu}}$
η - μ	(η, μ, \hat{r})	$M = 4\mu; K = 0; P = 1; \alpha = 2;$ $\sigma_i = \left[\frac{\eta\hat{r}^2}{2\mu(\eta+1)}\right]^{\frac{1}{2}}, \forall i \in \left\{1, \dots, \frac{M}{2}\right\};$ $\sigma_i = \left[\frac{\hat{r}^2}{2\mu(\eta+1)}\right]^{\frac{1}{2}}, \forall i \in \left\{\frac{M}{2} + 1, \dots, M\right\}.$	2μ	$\frac{\nu\hat{r}^2}{2} \left[\frac{4\sqrt{\pi}\eta^\mu\Gamma(2\mu)}{\mu^{2\mu-1}(\eta+1)^{2\mu}\Gamma(2\mu + \frac{1}{2})}\right]^{\frac{1}{2\mu}}$	$\frac{\hat{r}^2}{\gamma_{th}} \left[\frac{2\eta^\mu\Gamma(2\mu)}{\mu^{2\mu-1}(\eta+1)^{2\mu}}\right]^{\frac{1}{2\mu}}$
κ - μ	(κ, μ, \hat{r})	$M = 2\mu; K = \kappa; P = 1; \alpha = 2;$ $\sigma_i = \left[\frac{\hat{r}^2}{2\mu(\kappa+1)}\right]^{\frac{1}{2}}, \forall i \in \{1, \dots, M\}.$	μ	$\frac{\nu\hat{r}^2}{2} \left[\frac{2\sqrt{\pi}\Gamma(\mu)\exp[\kappa\mu]}{\mu^{\mu-1}(\kappa+1)^\mu\Gamma(\mu + \frac{1}{2})}\right]^{\frac{1}{\mu}}$	$\frac{\hat{r}^2}{\gamma_{th}} \left[\frac{\Gamma(\mu)\exp[\kappa\mu]}{\mu^{\mu-1}(\kappa+1)^\mu}\right]^{\frac{1}{\mu}}$
η - κ (Beckmann)	(η, κ, \hat{r})	$M = 2; K = \kappa; P = 1; \alpha = 2;$ $\sigma_1 = \left[\frac{\eta\hat{r}^2}{(\eta+1)(\kappa+1)}\right]^{\frac{1}{2}};$ $\sigma_2 = \left[\frac{\hat{r}^2}{(\eta+1)(\kappa+1)}\right]^{\frac{1}{2}}.$	1	$\nu\hat{r}^2 \frac{4\sqrt{\eta}\exp\left[\frac{\kappa(\eta+1)(q+1)}{2(\eta q+1)}\right]}{(\eta+1)(\kappa+1)}$	$\frac{\hat{r}^2}{\gamma_{th}} \frac{2\sqrt{\eta}\exp\left[\frac{\kappa(\eta+1)(q+1)}{2(\eta q+1)}\right]}{(\eta+1)(\kappa+1)}$
α - η - μ	$(\alpha, \eta, \mu, \hat{r})$	$M = 4\mu; K = 0; P = 1;$ $\sigma_i = \left[\frac{\eta\hat{r}^\alpha}{2\mu(\eta+1)}\right]^{\frac{1}{2}}, \forall i \in \left\{1, \dots, \frac{M}{2}\right\};$ $\sigma_i = \left[\frac{\hat{r}^\alpha}{2\mu(\eta+1)}\right]^{\frac{1}{2}}, \forall i \in \left\{\frac{M}{2} + 1, \dots, M\right\}.$	$\alpha\mu$	$\frac{\nu\hat{r}^2}{2} \left[\frac{4\sqrt{\pi}\mu^{1-2\mu}\eta^\mu\Gamma(2\mu)}{(\eta+1)^{2\mu}\Gamma(\alpha\mu + \frac{1}{2})}\right]^{\frac{1}{\alpha\mu}}$	$\frac{\hat{r}^2}{\gamma_{th}} \left[\frac{2\eta^\mu\Gamma(2\mu)}{\mu^{2\mu-1}(\eta+1)^{2\mu}}\right]^{\frac{1}{\alpha\mu}}$
α - κ - μ	$(\alpha, \kappa, \mu, \hat{r})$	$M = 2\mu; K = \kappa; P = 1; Q = q;$ $\sigma_i = \left[\frac{\hat{r}^\alpha}{2\mu(\kappa+1)}\right]^{\frac{1}{2}}, \forall i \in \{1, \dots, M\}.$	$\frac{\alpha\mu}{2}$	$\frac{\nu\hat{r}^2}{2} \left[\frac{2\sqrt{\pi}\mu^{1-\mu}\Gamma(\mu)\exp[\kappa\mu]}{(\kappa+1)^\mu\Gamma(\frac{\alpha\mu}{2} + \frac{1}{2})}\right]^{\frac{2}{\alpha\mu}}$	$\frac{\hat{r}^2}{\gamma_{th}} \left[\frac{\Gamma(\mu)\exp[\kappa\mu]}{\mu^{\mu-1}(\kappa+1)^\mu}\right]^{\frac{2}{\alpha\mu}}$
α - η - κ - μ	$(\alpha, \eta, \kappa, \mu, p, q, \hat{r})$	$M = 2\mu; K = \kappa; P = p; Q = q;$ $\sigma_i = \left[\frac{\eta\hat{r}^\alpha \left(\frac{p+1}{\eta+1}\right)}{2\mu p(\kappa+1)}\right]^{\frac{1}{2}}, \forall i \in \{1, \dots, M_x\};$ $\sigma_i = \left[\frac{\hat{r}^\alpha \left(\frac{p+1}{\eta+1}\right)}{2\mu(\kappa+1)}\right]^{\frac{1}{2}}, \forall i \in \{M_x + 1, \dots, M_x + M_y = M\}.$	$\frac{\alpha\mu}{2}$	$\frac{\nu\hat{r}^2}{2} \left\{ \frac{2\sqrt{\pi}(p+1)^\mu \left(\frac{\eta}{p}\right)^{\frac{p\mu}{p+1}}}{\mu^{\mu-1}(\eta+1)^\mu(\kappa+1)^\mu} \times \frac{\Gamma(\mu)\exp\left[\frac{\kappa\mu(\eta+1)(pq+1)}{(p+1)(\eta q+1)}\right]}{\Gamma\left(\frac{\alpha\mu}{2} + \frac{1}{2}\right)} \right\}^{\frac{2}{\alpha\mu}}$	$\frac{\hat{r}^2}{\gamma_{th}} \left\{ \frac{(p+1)^\mu \left(\frac{\eta}{p}\right)^{\frac{p\mu}{p+1}} \Gamma(\mu)}{\mu^{\mu-1}(\eta+1)^\mu(\kappa+1)^\mu} \times \exp\left[\frac{\kappa\mu(\eta+1)(pq+1)}{(p+1)(\eta q+1)}\right] \right\}^{\frac{2}{\alpha\mu}}$

^a See [7, Sec. VI] for further details on the original parameterization of the existing fading models.

V. APPLICATION TO MAXIMAL-RATIO COMBINING

MRC is a combining technique that has been widely exploited to improve the wireless system performance. This technique achieves full diversity order at high SNR and is optimum in the sense that it maximizes the output SNR for independent AWGN channels [14], [20]. Herein, we further extend our analysis in order to evaluate the performance of multibranch MRC receivers over generalized Gaussian-class fading.

Considering an MRC receiver with L mutually independent branches, let γ_l and γ_Σ represent the instantaneous SNR for the l th branch and for the combiner output, respectively. The resulting SNR γ_Σ is the sum of the SNRs of each individual branch [14], i.e.,

$$\gamma_\Sigma = \sum_{l=1}^L \gamma_l. \quad (26)$$

For convenience, let G_{d_l} and O_{d_l} denote the diversity gains of SEP and OP at the l th branch, and let G_{d_Σ} and O_{d_Σ} denote the resulting diversity gains of SEP and OP at the MRC output, respectively. As already observed in the literature, the resulting diversity gains of SEP and OP are given by [11]

$$G_{d_\Sigma} = \sum_{l=1}^L G_{d_l} \quad (27)$$

$$O_{d_\Sigma} = \sum_{l=1}^L O_{d_l}. \quad (28)$$

Furthermore, note from (21a) that the diversity gains of SEP and OP at the l th branch are identical, i.e., $G_{d_l} = O_{d_l}, \forall l$. Let α_l and M_l represent the nonlinearity parameter and the number of Gaussian clusters for the l th branch, respectively, such that (20a) and (21a) can be written as

$$G_{d_l} = O_{d_l} = \frac{\alpha_l M_l}{4}. \quad (29)$$

Therefore, substituting (29) into (27) and (28) we attain

$$G_{d_\Sigma} = O_{d_\Sigma} = \frac{1}{4} \sum_{l=1}^L \alpha_l M_l. \quad (30)$$

Similarly, let G_{c_l} and O_{c_l} denote the coding gains of SEP and OP at the l th branch, and let G_{c_Σ} and O_{c_Σ} denote the resulting coding gains of SEP and OP at the MRC output,

respectively. The resulting coding gains of SEP and OP can be obtained as [11]

$$G_{c_\Sigma} = \left\{ \frac{2^{L-1} \pi^{\frac{L-1}{2}} \Gamma\left(\frac{1}{2} + \sum_{l=1}^L G_{d_l}\right) \left[\prod_{l=1}^L G_{d_l} \Gamma(G_{d_l}) \right]}{\left(\sum_{l=1}^L G_{d_l} \right) \Gamma\left(\sum_{l=1}^L G_{d_l} \right)} \times \left[\prod_{l=1}^L \frac{1}{G_{c_l}^{G_{d_l}} \Gamma(G_{d_l} + \frac{1}{2})} \right] \right\}^{-\frac{1}{\sum_{l=1}^L G_{d_l}}} \quad (31a)$$

$$O_{c_\Sigma} = \left\{ \frac{\left[\prod_{l=1}^L O_{d_l} \Gamma(O_{d_l}) \right]}{\left(\sum_{l=1}^L O_{d_l} \right) \Gamma\left(\sum_{l=1}^L O_{d_l} \right) \left[\prod_{l=1}^L O_{c_l}^{O_{d_l}} \right]} \right\}^{-\frac{1}{\sum_{l=1}^L O_{d_l}}}. \quad (31b)$$

Also, recalling that α_l and M_l represent the nonlinearity parameter and the number of Gaussian clusters for the l th branch, respectively, we can rewrite (20b) and (21b) as

$$G_{c_l} = \nu \left\{ M_l \pi^{\frac{1}{2}} 2^{\frac{M_l}{2}(1-\frac{\alpha}{2})} \Gamma\left(\frac{M_l}{2}\right) \left[\Gamma\left(\frac{\alpha_l M_l}{4} + \frac{1}{2}\right) \right]^{-1} \times \exp \left[\frac{1}{2} \sum_{i=1}^{M_l} k_{l,i} \right] \prod_{i=1}^{M_l} \sigma_{l,i} \right\}^{\frac{4}{\alpha_l M_l}} \quad (32)$$

$$O_{c_l} = \frac{1}{\gamma_{th}} \left\{ \frac{M_l}{2^{1-\frac{M_l}{2}}} \Gamma\left(\frac{M_l}{2}\right) \exp \left[\frac{1}{2} \sum_{i=1}^{M_l} k_{l,i} \right] \prod_{i=1}^{M_l} \sigma_{l,i} \right\}^{\frac{4}{\alpha_l M_l}}, \quad (33)$$

where $\sigma_{l,i}$ and $k_{l,i}$ are the standard deviation and the power ratio, respectively, for the i th cluster of the l th branch. We can then substitute (32) and (33) into (31a) and (31b), respectively, so as to obtain the resulting coding gains in (34) and (35), shown at the bottom of this page.

Note that the closed-form expressions obtained in (30), (34), and (35) are novel and fully describe the asymptotic performance of MRC receivers operating over a large variety of Gaussian-class fading channels.

VI. NUMERICAL RESULTS

In this section, we evaluate how the diversity and coding gains vary with the fading parameters M , σ , k , and α for single-branch and multibranch MRC receivers. We have extensively validated our asymptotic expressions by comparing them with their corresponding exact solutions, obtained via

$$G_{c_\Sigma} = \nu \left\{ \frac{2^{L-1} \pi^{\frac{1}{2}} \prod_{l=1}^L 2^{\frac{M_l}{2}(1-\frac{\alpha_l}{2})} \Gamma\left(\frac{M_l}{2}\right) \exp \left[\frac{1}{2} \sum_{i=1}^{M_l} k_{l,i} \right] \prod_{i=1}^{M_l} \sigma_{l,i}}{\left[\left(\sum_{l=1}^L \alpha_l M_l \right) \Gamma\left(\frac{1}{4} \sum_{l=1}^L \alpha_l M_l\right) \right]^{-1} \Gamma\left(\frac{1}{2} + \frac{1}{4} \sum_{l=1}^L \alpha_l M_l\right) \prod_{l=1}^L \alpha_l \Gamma\left(\frac{\alpha_l M_l}{4}\right)} \right\}^{\frac{4}{\sum_{l=1}^L \alpha_l M_l}} \quad (34)$$

$$O_{c_\Sigma} = \frac{1}{\gamma_{th}} \left\{ \frac{2^{L-2} \prod_{l=1}^L 2^{\frac{M_l}{2}} \Gamma\left(\frac{M_l}{2}\right) \exp \left[\frac{1}{2} \sum_{i=1}^{M_l} k_{l,i} \right] \prod_{i=1}^{M_l} \sigma_{l,i}}{\left[\left(\sum_{l=1}^L \alpha_l M_l \right) \Gamma\left(\frac{1}{4} \sum_{l=1}^L \alpha_l M_l\right) \right]^{-1} \prod_{l=1}^L \alpha_l \Gamma\left(\frac{\alpha_l M_l}{4}\right)} \right\}^{\frac{4}{\sum_{l=1}^L \alpha_l M_l}} \quad (35)$$

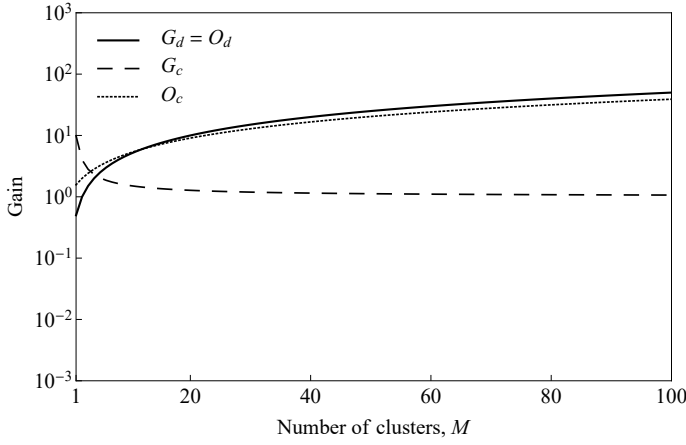


Fig. 1. Diversity and coding gains as a function of the number of clusters for $\alpha = 2$, $\sigma = 1$, and $k = 0$.

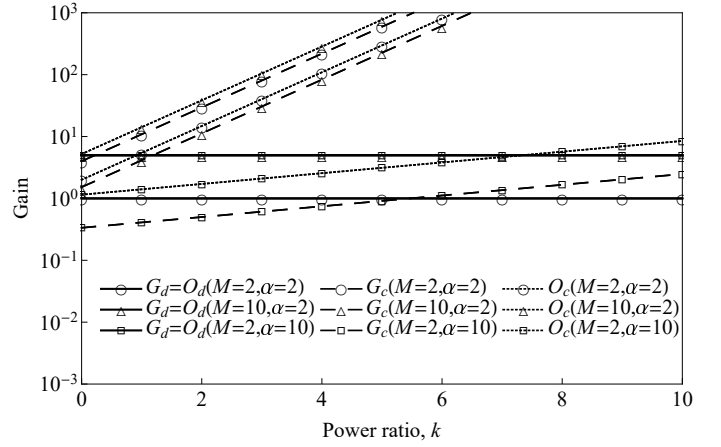


Fig. 3. Diversity and coding gains as a function of the power ratio for $\sigma = 1$ and some combinations of M and α .

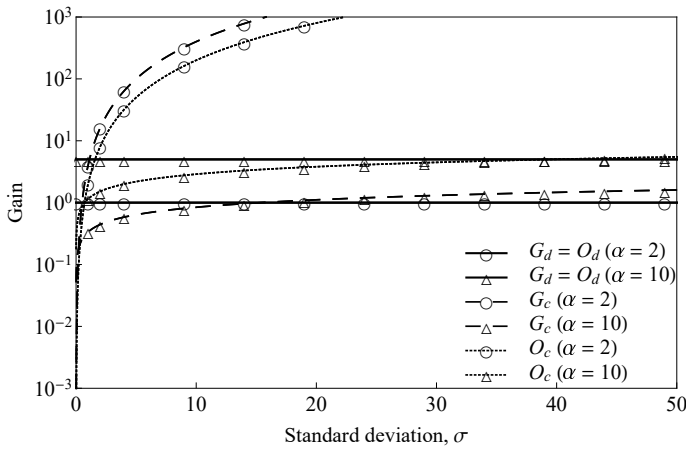


Fig. 2. Diversity and coding gains as a function of the standard deviation for varying α , $M = 2$, and $k = 0$.

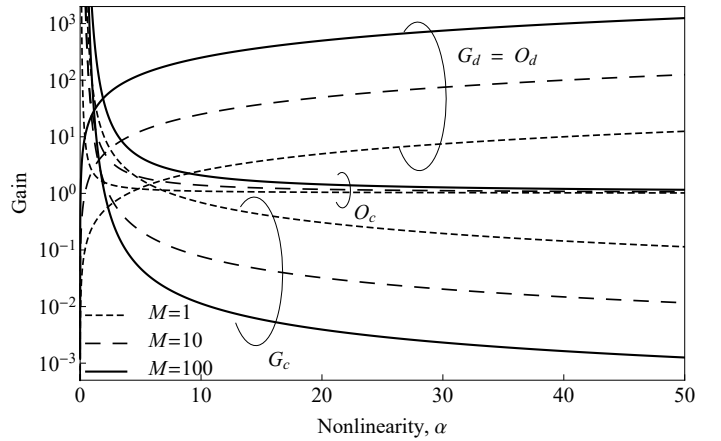


Fig. 4. Diversity and coding gains as a function of the nonlinearity for varying M , $\sigma = 1$, and $k = 0$.

numerical integration using the software Mathematica. For illustrative purposes, we consider the commutative scenario and let $M_l = M$, $\sigma_l = \sigma$, $k_l = k$, and $\alpha_l = \alpha$, $\forall l$, with $\nu = \gamma_{\text{th}} = 1$. In particular, $M = 2$ represents popular fading models such as Rayleigh, Rice, Hoyt, and Weibull; $\sigma = 1$, scattered waves of unit powers; $k = 0$, absence of line of sight; and $\alpha = 2$ and $\alpha \neq 2$, linear and nonlinear media, respectively.

A. Single-Branch Receivers

The analysis for the diversity gain is quite simple: note from (22a) that G_d and O_d are directly proportional to the medium nonlinearity (α) and to the number of clusters (M). This indicates that as α and M increase, so does the magnitude of the slope in the SEP and OP curves, as expected from (2) and (4). Therefore, the fading parameters α and M increase the diversity gain, as illustrated in Figs. 1–4, and ultimately dominate the system performance at high SNR.

The analysis for the coding gains is more cumbersome. Figs. 1–4 depict the coding gains in terms of M , σ , k , and α , respectively. As M increases, Fig. 1 shows that O_c increases and, more interestingly, G_c decreases. However, this

does not necessarily mean that the SEP increases, since the diversity gain $G_d = \frac{\alpha M}{4}$ increases with M , and this latter aspect dominates the system performance at high SNR, as already mentioned. In Fig. 2, σ increases the coding gains by $(40/\alpha) \log[\sigma]$ dB, and in Fig. 3, k increases them by $20(k/\alpha) \log[e]$ dB, where e is the Euler's number. These three figures reveal that a growth in the number of multipath clusters (M), in the power of scattered waves (σ^2), or in the power of specular components (m^2) improves the system performance. Indeed, such growth corresponds to more signal replicas (M) or signal power (σ^2 and m^2) reaching the receiver, thereby decreasing metrics such as SER and OP. In Fig. 4, the coding gains approach infinity as α approaches zero, a region that corresponds to a severe fading condition [7]. Conversely, as α increases, O_c approaches unity (zero decibel) and G_c approaches zero. In this case, even though G_c tends to deteriorate the channel as α approaches infinity, note that $G_d = \frac{\alpha M}{4}$ is also a function of α , which dominates the SEP at high SNR. Hence, the system performance improves when the parameters M , σ , m , and α increase, a result that corroborates and generalizes others recently obtained in the literature for particular fading models, e.g., the α - η - μ [21] and the α - κ - μ [22] distributions.

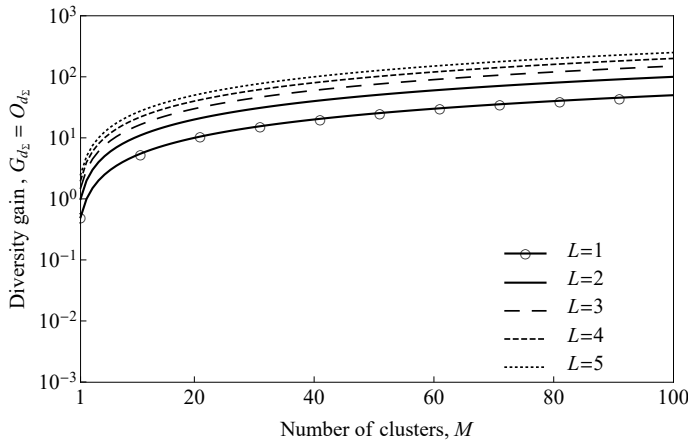


Fig. 5. MRC diversity gain as a function of the number of clusters for varying number of branches L , $\alpha = 2$, $\sigma = 1$, and $k = 0$.

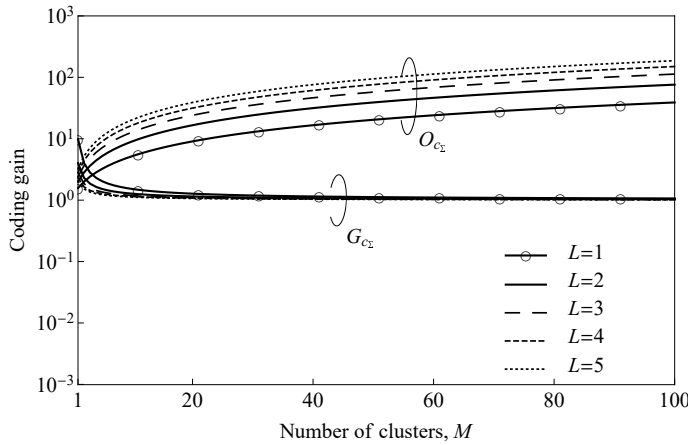


Fig. 6. MRC coding gains as a function of the number of clusters for varying number of branches L , $\alpha = 2$, $\sigma = 1$, and $k = 0$.

B. Multibranch Receivers

Herein we consider multibranch MRC receivers operating over the commutative scenario. As can be noticed from Figs. 5–11, the fading parameters impact such receivers in a similar fashion as that of the single-branch case. Therefore, in the following discussion we focus mainly on the impact of the number of branches on the system performance.

Note from (30) that the resulting diversity gains of SEP and OP are given as $G_{d_{\Sigma}} = O_{d_{\Sigma}} = \frac{1}{4} \sum_{l=1}^L \alpha_l M_l$, i.e., when L increases, so do $G_{d_{\Sigma}}$ and $O_{d_{\Sigma}}$. In particular, when $\alpha_l = \alpha$ and $M_l = M$, $\forall l$, the resulting diversity gains are given by $G_{d_{\Sigma}} = O_{d_{\Sigma}} = \frac{\alpha LM}{4}$, which implies that (i) the diversity gains vary linearly with L , (ii) the diversity gains in the linear scenario ($\alpha = 2$) are half the total number of Gaussian clusters ($G_{d_{\Sigma}} = O_{d_{\Sigma}} = \frac{LM}{2}$), and (iii) the number of branches (L) is interchangeable with the number of Gaussian clusters per branch (M), causing an equivalent impact on diversity.

The coding gains of SEP and OP have different behaviors as L varies: when L increases, $O_{c_{\Sigma}}$ also increases, but $G_{c_{\Sigma}}$ decreases, as shown in Figs. 6–11. Unlike for the diversity gains, these variations are no longer linear with L . In particular, on a log scale (or, equivalently, on a dB basis), the variations in the

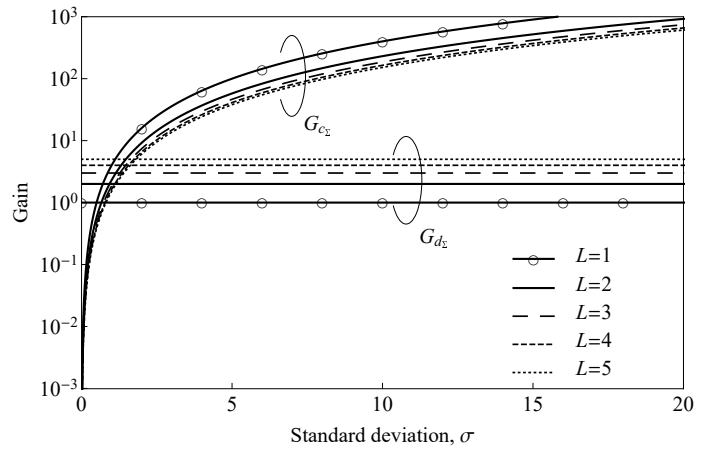


Fig. 7. MRC diversity and coding gains of SEP as a function of the standard deviation for varying number of branches L , $\alpha = 2$, $M = 2$, and $k = 0$.

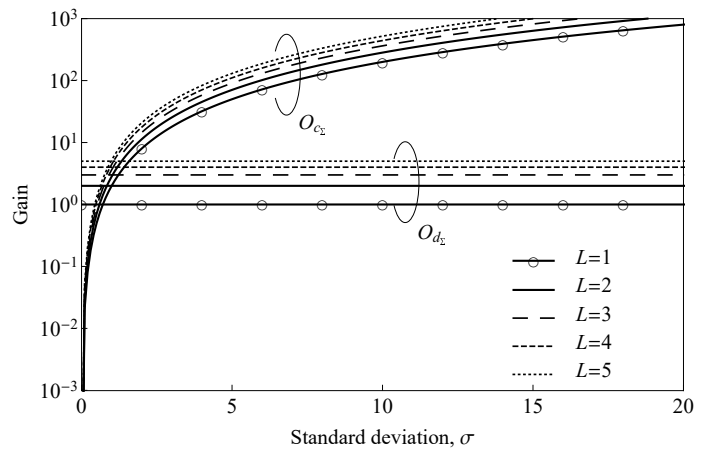


Fig. 8. MRC diversity and coding gains of OP as a function of the standard deviation for varying number of branches L , $\alpha = 2$, $M = 2$, and $k = 0$.

coding gains are seen to diminish as L increases. Also note in Fig. 11 that the coding gain of SEP tends to zero when α increases, regardless of L . However, as already mentioned for the single-branch receiver, the diversity gain dominates the system performance at sufficiently high SNR, and hence the SEP decreases when α increases.

These insights are useful to determine in a simple manner the high-SNR performance of MRC receivers operating over a broad class of fading models.

VII. CONCLUSIONS

In this work we proposed a simple and unified asymptotic performance analysis of communications systems operating over fading channels. Closed-form expressions for the diversity and coding gains of SEP and OP were derived considering a general fading model that covers a multitude of propagation scenarios. Such analysis offers insights on how each fading parameter affects the wireless system performance at high-SNR regime. We also further extended the results to investigate the performance of MRC receivers. It turned out that all the referred fading aspects affect the coding gains, whereas only the clustering and nonlinearity affect the diversity gain.

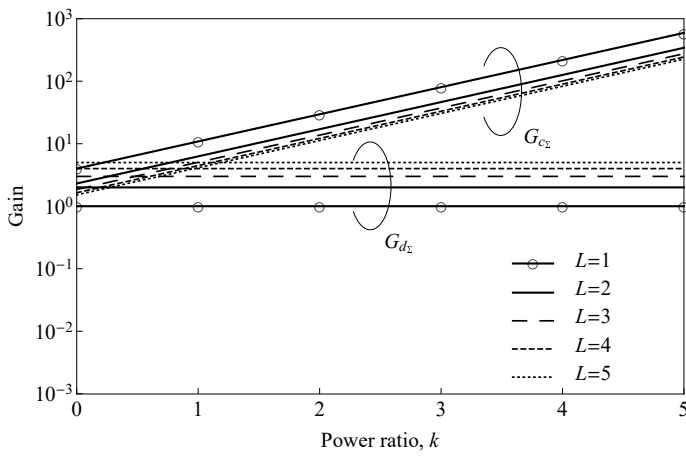


Fig. 9. MRC diversity and coding gains of SEP as a function of the power ratio for varying number of branches L , $\alpha = 2$, $M = 2$, and $\sigma = 1$.

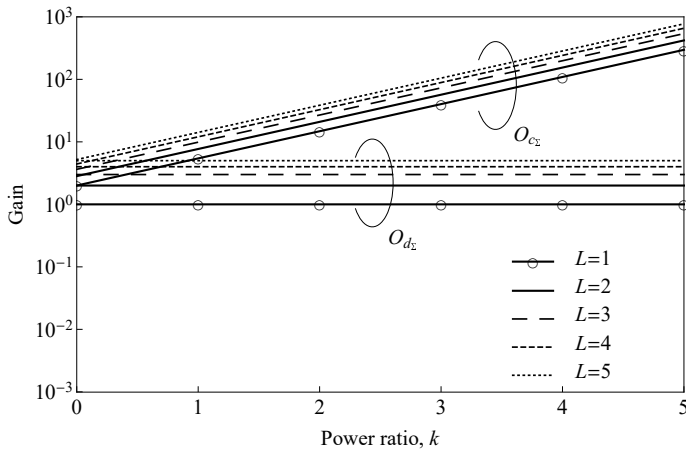


Fig. 10. MRC diversity and coding gains of OP as a function of the power ratio for varying number of branches L , $\alpha = 2$, $M = 2$, and $\sigma = 1$.

This can be readily used to evaluate many communication schemes operating in a broad family of propagation scenarios, thus helping optimize system design.

REFERENCES

[1] F. R. A. Parente, F. P. Calmon, and J. C. S. Santos Filho, "Unified asymptotic performance of communication systems in fading channels," in *Proc. XXXVII Brazilian Symp. Telecommun. Signal Process. (SBrT'19)*, Petrópolis, RJ, Brazil, Sep./Oct., 2019, doi: 10.14209/SBRT.2019.1570559219.

[2] P. C. F. Eggers, M. Angjelichinoski, and P. Popovski, "Wireless channel modeling perspectives for ultra-reliable communications," *IEEE Trans. Wireless Commun.*, vol. 18, no. 4, pp. 2229–2243, Apr. 2019, doi: 10.1109/TWC.2019.2901788.

[3] H. Ji, S. Park, J. Yeo, Y. Kim, J. Lee, and B. Shim, "Ultra-reliable and low-latency communications in 5G downlink: Physical layer aspects," *IEEE Wireless Commun.*, vol. 25, no. 3, pp. 124–130, Jun. 2018, doi: 10.1109/MWC.2018.1700294.

[4] J. G. Andrews, S. Buzzi, W. Choi, S. V. Hanly, A. Lozano, A. C. K. Soong, and J. C. Zhang, "What will 5G be?" *IEEE J. Sel. Areas Commun.*, vol. 32, no. 6, pp. 1065–1082, Jun. 2014, doi: 10.1109/JSAC.2014.2328098.

[5] L. Bariah, S. Muhaidat, and A. Al-Dweik, "Error probability analysis of non-orthogonal multiple access over Nakagami- m fading channels," *IEEE Trans. Commun.*, vol. 67, no. 2, pp. 1586–1599, Feb. 2019, doi: 10.1109/TCOMM.2018.2876867.

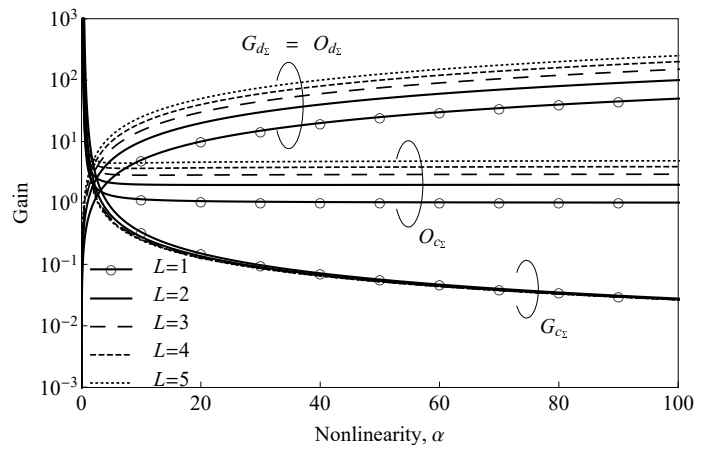


Fig. 11. MRC diversity and coding gains of SEP and OP as a function of the nonlinearity for varying number of branches L , $M = 2$, $\sigma = 1$, and $k = 0$.

[6] V. M. Baeza and A. G. Armada, "Non-coherent massive SIMO system based on M-DPSK for Rician channels," *IEEE Trans. Veh. Technol.*, vol. 68, no. 3, pp. 2413–2426, Mar. 2019, doi: 10.1109/TVT.2019.2892390.

[7] M. D. Yacoub, "The α - η - κ - μ fading model," *IEEE Trans. Antennas Propag.*, vol. 64, no. 8, pp. 3597–3610, Aug. 2016, doi: 10.1109/TAP.2016.2570235.

[8] J. Medbo, P. Kyosti, K. Kusume, L. Raschkowski, K. Haneda, T. Jamsa, V. Nurmela, A. Roivainen, and J. Meinila, "Radio propagation modeling for 5G mobile and wireless communications," *IEEE Commun. Mag.*, vol. 54, no. 6, pp. 144–151, Jun. 2016, doi: 10.1109/MCOM.2016.7498102.

[9] F. R. A. Parente and J. C. S. Santos Filho, "Asymptotically exact framework to approximate sums of positive correlated random variables and application to diversity-combining receivers," *IEEE Wireless Commun. Lett.*, vol. 8, no. 4, pp. 1012–1015, Aug. 2019, doi: 10.1109/LWC.2019.2904032.

[10] B. Zhu, J. Yan, Y. Wang, L. Wu, and J. Cheng, "Asymptotically tight performance bounds of diversity receptions over α - μ fading channels with arbitrary correlation," *IEEE Trans. Veh. Technol.*, vol. 66, no. 9, pp. 7619–7632, Sep. 2017, doi: 10.1109/TVT.2017.2686700.

[11] Z. Wang and G. B. Giannakis, "A simple and general parameterization quantifying performance in fading channels," *IEEE Trans. Commun.*, vol. 51, no. 8, pp. 1389–1398, Aug. 2003, doi: 10.1109/TCOMM.2003.815053.

[12] Y. H. Al-Badarnah, C. N. Georgeghiadis, and M. Alouini, "Asymptotic performance analysis of the k th best link selection over wireless fading channels: An extreme value theory approach," *IEEE Trans. Veh. Technol.*, vol. 67, no. 7, pp. 6652–6657, Jul. 2018, doi: 10.1109/TVT.2018.2798501.

[13] X. Song, J. Cheng, and N. C. Beaulieu, "Asymptotic analysis of different multibranch diversity receivers with arbitrarily correlated Rician channels," *IEEE Trans. Wireless Commun.*, vol. 13, no. 10, pp. 5676–5689, Oct. 2014, doi: 10.1109/TWC.2014.2328993.

[14] A. Goldsmith, *Wireless Communications*. New York: Cambridge University Press, 2005, doi: 10.1017/CBO9780511841224.

[15] Y. S. Chow and H. Teicher, *Probability Theory: Independence, Interchangeability, Martingales*, 3rd ed. New York: Springer, 2003, doi: 10.1007/978-1-4612-1950-7.

[16] A. F. Molisch, *Wireless Communications*, 2nd ed. New York: Wiley, 2011.

[17] N. C. Beaulieu and K. T. Hemachandra, "Novel simple representations for Gaussian class multivariate distributions with generalized correlation," *IEEE Trans. Inf. Theory*, vol. 57, no. 12, pp. 8072–8083, Dec. 2011, doi: 10.1109/TIT.2011.2170133.

[18] M. Nakagami, "The m -distribution – A general formula of intensity distribution of rapid fading," in *Statistical Methods in Radio Wave Propagation*, W. C. Hoffman, Ed. Oxford, U.K.: Pergamon, 1960, pp. 3–36, doi: 10.1016/B978-0-08-009306-2.50005-4.

[19] V. Perim, J. D. V. Sánchez, and J. C. S. Santos Filho, "Asymptotically exact approximations to generalized fading sum statistics," *IEEE Trans. Wireless Commun.*, vol. 19, no. 1, pp. 205–217, Jan. 2020, doi: 10.1109/TWC.2019.2943336.

- [20] M. Rodríguez, R. Feick, R. A. Valenzuela, and D. Chizhik, "Achieving near maximum ratio combining diversity gains with directive antennas," *IEEE Trans. Veh. Technol.*, vol. 66, no. 9, pp. 7782–7796, Sep. 2017, doi: 10.1109/TVT.2017.2684079.
- [21] O. S. Badarneh and M. S. Aloiqlah, "Performance analysis of digital communication systems over α - η - μ fading channels," *IEEE Trans. Veh. Technol.*, vol. 65, no. 10, pp. 7972–7981, Oct. 2016, doi: 10.1109/TVT.2015.2504381.
- [22] J. M. Moualeu, D. B. da Costa, W. Hamouda, U. S. Dias, and R. A. A. de Souza, "Performance analysis of digital communication systems over α - κ - μ fading channels," *IEEE Commun. Lett.*, vol. 23, no. 1, pp. 192–195, Jan. 2019, doi: 10.1109/LCOMM.2018.2878218.



Francisco Raimundo Albuquerque Parente (S'19) received the B.Sc. degree in Computer Engineering from Federal University of Ceará (UFC), CE, Brazil, in 2016, and the M.Sc. degree in Electrical Engineering from University of Campinas (UNICAMP), SP, Brazil, in 2019. From 2014 to 2015, he was an international scholarship recipient to study and develop research in the College of Engineering of Temple University, PA, USA. He is currently a Ph.D. candidate in Electrical Engineering in the Department of Communications,

School of Electrical and Computer Engineering, UNICAMP. His research areas include asymptotic theory, statistics, wireless communications, and optical systems.



Flavio du Pin Calmon is an Assistant Professor of Electrical Engineering at Harvard's John A. Paulson School of Engineering and Applied Sciences. Before joining Harvard, he was the inaugural data science for social good post-doctoral fellow at IBM Research in Yorktown Heights, New York. He received his Ph.D. in Electrical Engineering and Computer Science at MIT. His main research interests are information theory, inference, and statistics, with applications to fairness, privacy, machine learning, and communications engineering. Prof. Calmon has

received the NSF CAREER award, the Google Research Faculty Award, the IBM Open Collaborative Research Award, and Harvard's Lemann Brazil Research Fund Award.



José Cândido Silveira Santos Filho (M'09) received the B.Sc., M.Sc., and Ph.D. degrees from the School of Electrical and Computer Engineering (FEEC), University of Campinas (UNICAMP), Campinas, SP, Brazil, in 2001, 2003, and 2006, respectively, all in electrical engineering. He was ranked first in his undergraduate program, and his Ph.D. thesis was awarded an Honorary Mention by the Brazilian Ministry of Education (CAPES) in the 2007 CAPES Thesis Contest. From 2006 to 2009, he was a Post-Doctoral Fellow with the Wireless

Technology Laboratory, FEEC-UNICAMP. He is currently an Assistant Professor with FEEC-UNICAMP. Since 2011, he has been regularly consulted for Bradar Indústria S.A., a branch of Embraer Defense and Security, in the development of innovative radar techniques. From June 2018 to September 2019, he served as a visiting researcher at Harvard University. He has authored over 100 technical papers, about half of which in international journals, and has served as a reviewer for many journals and conferences. His research areas include wireless communications and radar systems.